Los Alamos
NATIONAL LABORATORY
EST.1943

LA-UR-17-29435
Approved for public release; distribution is unlimited.

Title: SAVY-4000 O-Ring and Filter Lifetime Extension Report

Author(s): Welch, Cynthia F.; Weis, Eric; Smith, Paul Herrick; Stone, Timothy Amos; Reeves, Kirk Patrick; Karns, Tristan; Oka, Jude M.; Keller, Jennie; Herman, Matthew Joseph; Weaver, Brian Phillip; Adams, Jillian Cathleen; Trautschold, Olivia Carol; Van Buskirk, Caleb Griffith; Garcia, Michael David

Intended for: Report

Issued: 2018-07-30 (rev.1)

Disclaimer:
Los Alamos National Laboratory, an affirmative action/equal opportunity employer, is operated by the Los Alamos National Security, LLC for the National Nuclear Security Administration of the U.S. Department of Energy under contract DE-AC52-06NA25396. By approving this article, the publisher recognizes that the U.S. Government retains nonexclusive, royalty-free license to publish or reproduce the published form of this contribution, or to allow others to do so, for U.S. Government purposes. Los Alamos National Laboratory requests that the publisher identify this article as work performed under the auspices of the U.S. Department of Energy. Los Alamos National Laboratory strongly supports academic freedom and a researcher's right to publish; as an institution, however, the Laboratory does not endorse the viewpoint of a publication or guarantee its technical correctness.

SAVY-4000 O-Ring and Filter Lifetime Extension Report

Cynthia F. Welch (MST-7)
Eric M. Weis (MST-7)
Paul H. Smith (NPI-2)
Tim A. Stone (NPI-2)
Kirk P. Reeves (NPI-2)
Tristan Karns (NPI-2)
Jude M. Oka (NPI-2)
Jennie Keller (MST-7)
Matthew J. Herman (MST-7)
Brian Weaver (CCS-6)
Jillian C. Adams (MST-7)
Olivia C. Trautschold (MST-7)
Caleb Van Buskirk (MST-7)
Michael Garcia (MST-7)

1 Executive Summary

The 3-year accelerated aging study of the SAVY-4000 O-ring detailed in our previous Lifetime Extension Report showed very little evidence of significant degradation to samples subjected to aggressive elevated temperature and radiation conditions. Whole container thermal aging studies followed by helium leakage testing and compression set measurements were used to establish a failure criterion estimate for O-ring compression set of ≥65 %, which led to an O-ring lifetime estimate of greater than 65 years at 80°C. Herein, we describe a statistical model of the 3-year accelerated aging study and present additional results gathered in FY17 that further support the lifetime extension of the O-ring to 40 years at 80°C. Because we are choosing an extremely conservative lifetime value (40 years) compared to the aging study results (>65 years), the O-ring lifetime could be extended further, especially if supported by surveillance results collected over the years to come.

2 Introduction

The Department of Energy (DOE) issued DOE M 441.1-1, Nuclear Material Packaging Manual, in March 2008, to protect workers who handle nuclear material from exposure due to loss of containment of stored materials.[1] The manual specifies a detailed approach to achieve high confidence in containers and includes requirements for container design and performance, design-life determinations, material contents, and surveillance and maintenance to ensure container integrity over time. In order to implement DOE M441.1-1, Nuclear Filter Technology, Inc. (NucFil) and LANL developed the SAVY-4000 container, named for the designers Stone, Anderson, Veirs, and Yarbro.[2] The SAVY-4000 design includes eight sizes (1-, 2-, 3-, 5-, 8-, 12-quart and 5- and 10-gallon), and they will replace the current "Hagan" style containers[3] of the same sizes. The SAVY-4000 is closed and sealed by pushing the lid downward into the collar resulting in radial compression of an O-ring between the body collar and a piston groove in the lid, as shown in Figure 2.1.

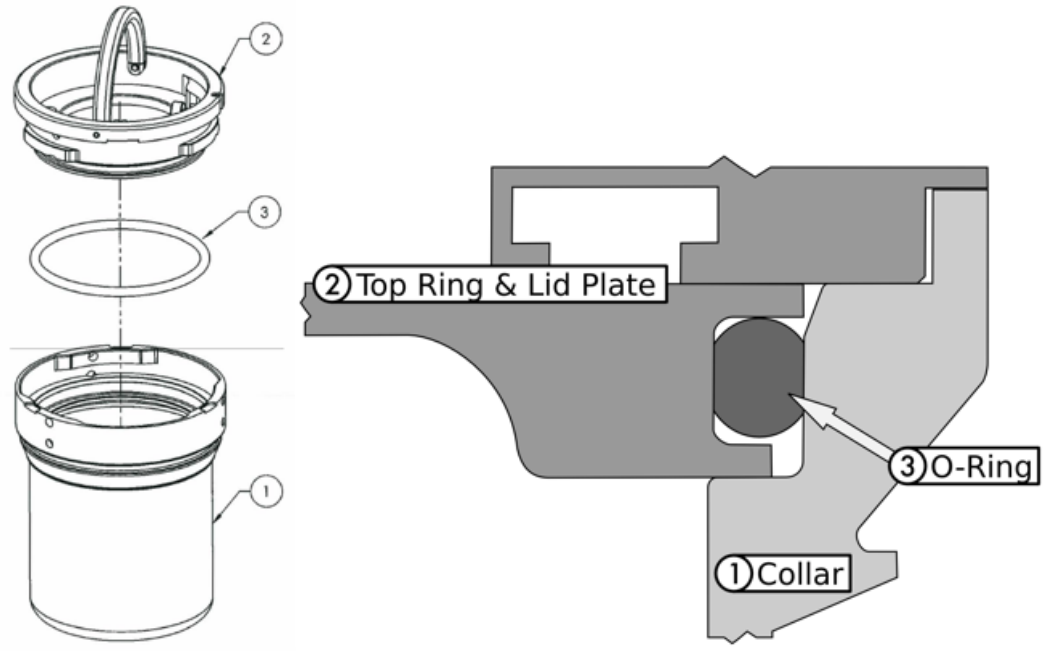

Figure 2.1. (a) SAVY-4000 container, showing (a2) the lid plate and top ring, (a3) O-ring, and (a1) container body with collar. (b) cross-sectional view of the O-ring installed in the lid in a closed container.

The O-ring used in the SAVY-4000 has been identified as one of the lifetime-limiting components of the design, and it is a part that is vulnerable to wear through repeated use. Preliminary studies detailed[3,4] the basic properties, composition and durability of the SAVY-4000 O-rings. However, the fluoropolymer-based O-ring may deteriorate over time due to compression, elevated temperatures, and exposure to ionizing radiation. These O-rings are a type of FKM rubber (like Viton®) purchased from Parker, Inc. In personal communication, a Parker quality control scientist further specified that the base polymer was a copolymer of hexafluoropropene (HFP) and vinylidene difluoride (VDF), which is known as Type 1 FKM.

In 2013, we developed an accelerated aging plan[5] to quantify changes, both chemical and physical, that the O-ring could display as a result of service conditions. The results of that accelerated aging study were detailed in a previous SAVY-4000 Lifetime Extension Report.[6] The current report gives an overview of those results plus a recently completed statistical model (Section 3) and provides details on additional experiments conducted in FY17 (Section 4). Current conclusions regarding lifetime are contained in Section 5.

3 Statistical Model of Previous Accelerated Aging Results

As described in a previous SAVY-4000 Lifetime Extension Report,[6] data collected during the 3-year accelerated thermal aging study suggested that as many as three aging mechanisms can cause compression set in the O-ring: a reversible one and two irreversible ones. Using various characterization techniques on aged samples, we only detected chemical degradation at the highest aging temperatures and longest aging times. To separate the effect of the reversible aging mechanism from the irreversible ones, we measured compression set after allowing the aged O-rings to physically relax for long periods of time. Compression set was reduced for samples aged at low temperatures (70 – 120°C), while at high aging temperatures (160 – 210°C) compression set was maintained. In FY16, the failure point of the compression set was chosen as 65% to reflect the results of the whole-container aging experiments. Using this criterion in conjunction with time-temperature superposition (via the visual inspection method) of the compression set data, we obtained two estimates for O-ring lifetime at 80°C. The first estimate used the high-temperature shift factors employed in the time-temperature superposition analysis to back-calculate new shift factors for the low temperature region (70 – 90°C). In this way, we obtained a lifetime due to the high-activation-energy irreversible process only. Using these new shift factors, we estimated a lifetime range of 267 to 39,675 years at 80°C. The second estimate reflected the combined effect of both irreversible processes to give a lifetime in the range of 65 to 9647 years at 80°C. In order to narrow these ranges and provide a firmer statistical basis for quantifying the uncertainty in them, we developed a statistical model that incorporates measurement error and preserves the constraints of the compression set measurement (i.e., results must range from 0% to 100%).

Figure 3.1 displays the compression set measurements for the full 3-year accelerated thermal aging study. Our analysis focuses on the data associated with aging temperatures of 160-210°C because these samples do not undergo the reversible aging mechanism.[6]

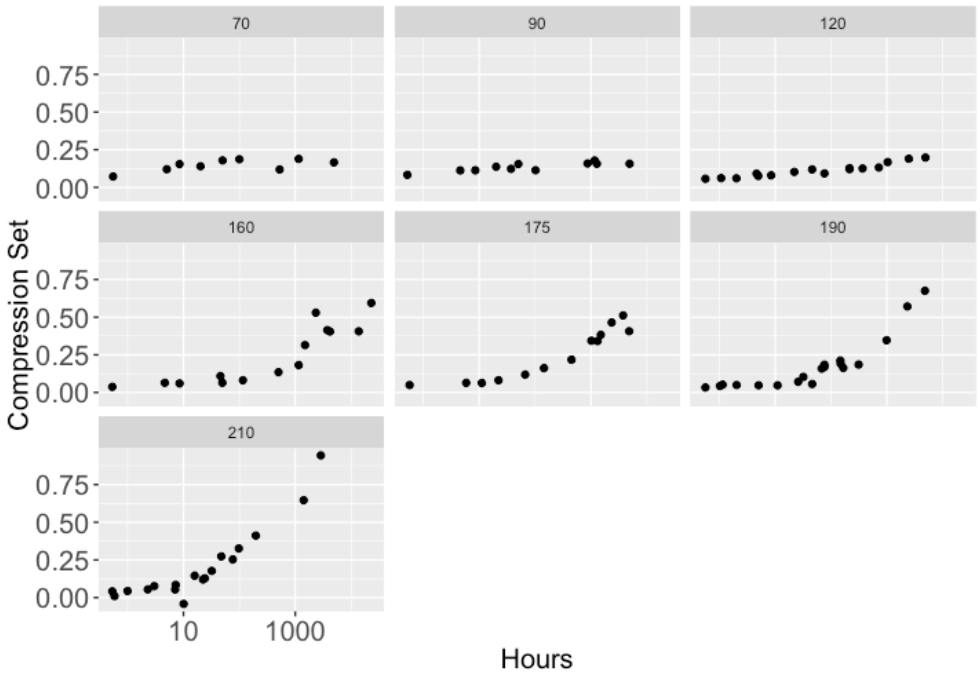

Figure 3.2: Compression set data from the 3-year accelerated thermal aging study.

Before we introduce our statistical model, we need to define some notation. C_B is our random variable associated with a compression set measurement, Y is some transformation of C_B, t is time, and Temp is temperature. We assume the following mathematical form for C_B:

$$C_B = \Phi\left(\frac{\ln(t) - \mu(\text{Temp})}{\sigma}\right),$$

where Φ is the error function (erf) or standard normal cumulative distribution function. The erf function is selected because it is bounded between 0 and 1 and allows for the type of shifts dictated by time-temperature superposition. In our function, σ controls the shape of C_B and μ controls its location. In particular, $\exp(\mu)$ gives the point in time yielding 50% C_B. The location of the C_B is shifted by temperature in the following way

$$\mu(\text{Temp}) = \beta_0 + \beta_1 \frac{1}{\text{Temp}} = \beta_0 + \beta_1 X,$$

where β_1 and β_0 are unknown parameters and are estimated from the data. For brevity in the notation we will use $\mu(\text{X})$ instead of $\mu(\text{Temp})$. A forthcoming report will provide more details on this formulation.

Notice that the C_B model can be rewritten into a linear model by applying the inverse of the erf function:

$$Y = \Phi^{-1}(C_B) = \frac{\ln(t) - \beta_0 + \beta_1 X}{\sigma} = \alpha_0 + \alpha_1 \ln(t) + \alpha_2 X.$$

Additionally, we add normal noise terms to complete our statistical model:

$$Y = \alpha_0 + \alpha_1 \ln(t) + \alpha_2 X + \varepsilon,$$

where $\varepsilon \sim N(0, \tau^2)$ and is interpreted as measurement error on *Y*. On this transformed scale, one can simply estimate the unknown parameters using ordinary least squares and use all of the corresponding statistical properties associated with that estimation method.

We fit our linear model to the 160-210°C C_B data. Figure 3.2 shows the fitted model along with 95% uncertainty intervals. The horizontal line present in each panel represents the 65% compression set failure criterion for the O-rings.

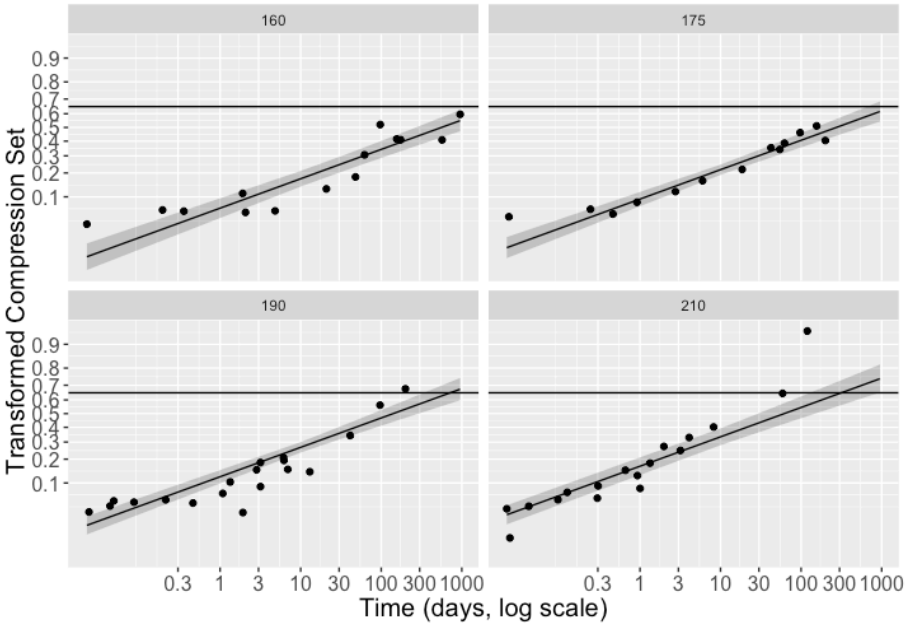

Figure 3.3: Model fit for the compression set data.

With this fitted model, we can make predictions of C_B at other temperatures. Surveillance data was taken on eleven SAVY containers stored at ambient temperature (25-35°C). Figure 3.3 shows our predictions (solid and dashed line) with corresponding prediction intervals (red and blue ribbons), based on the above model, for these surveillance units (dots with error bars). Notice that for both temperatures, the intervals capture the surveillance units.

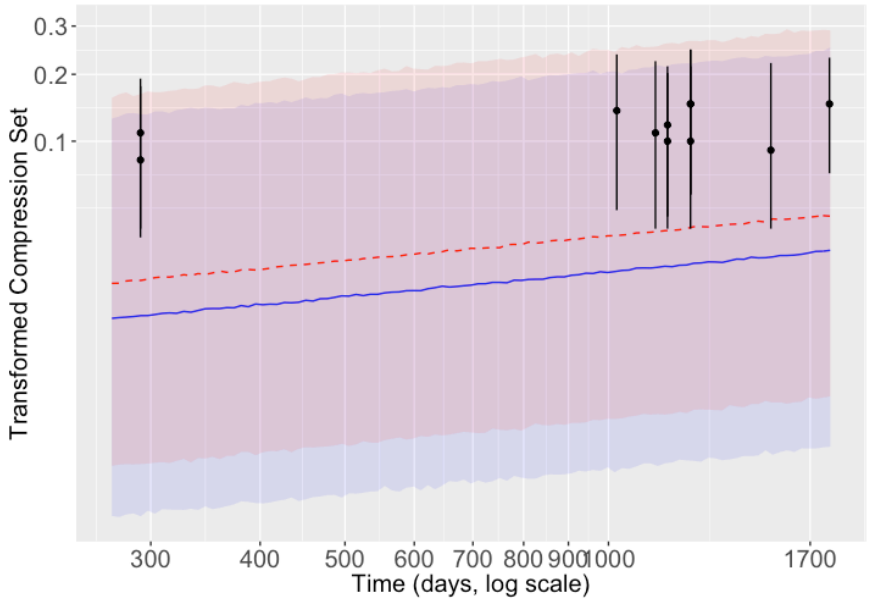

Figure 3.4: Model predictions with corresponding prediction interval of surveillance units. The red dashed line is 35°C and blue solid line is 25°C. Surveillance units are given as points.

Lastly, the estimated model is used to predict failure times for the O-rings. From the FY16 accelerated aging study, the C_B value yielding a failure is 0.65.[6] From the model, the formula for the failure time is found by solving for the point in time that gives a $C_B = 0.65$ value. This is calculated using

$$t_f = \exp[\mu(\mathrm{X}) + \Phi^{-1}(0.65)\sigma].$$

Figure 3.4 shows the estimated compression curve for 80°C (black line) along with its 95% uncertainty interval. The horizontal red line is the failure threshold. The O-rings are predicted to fail when this curve crosses the horizontal line. Using our time-to-failure formula predicts this to be about 993 years with a corresponding uncertainty interval of 68 to 15,000 years.

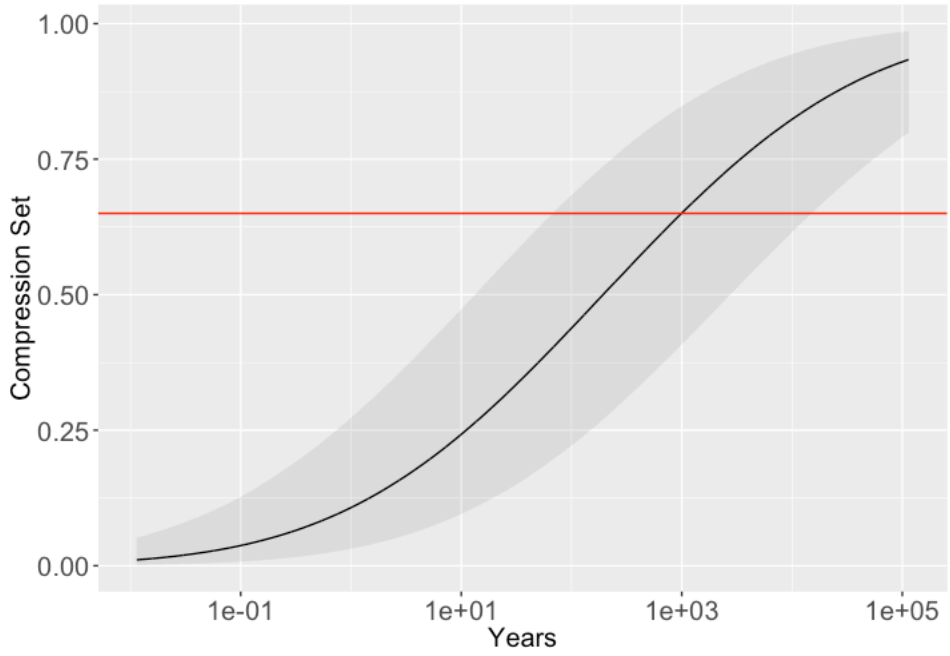

Figure 3.5: Predicted C_B curve for 80°C (black line) with corrsponding 95% uncertainty interval (gray ribbon). The red horizontal line is the failure threshold of 0.65.

4 FY17 Experimental Results

In addition to developing the statistical model described in Section 3, in FY17 we conducted some additional experiments aimed at obtaining a better understanding of the various degradation mechanisms. In Section 4.1, we describe additional whole container accelerated aging experiments that were conducted to better quantify the compression set at which the O-ring will fail the leak test. Section 4.2 discusses solvent-swelling experiments that provide insight into chemical degradation mechanisms that changed the extent of crosslinking during the thermal aging experiments. Section 4.3 gives an overview of an oxygen consumption study designed to reveal the effects of any oxidative degradation reactions that occur during thermal aging. Finally, Section 4.4 presents results from our synergistic effects experiments, in which samples received both elevated temperature and irradiation.

4.1 Whole-Container Thermal Aging Study

Whole container aging experiments conducted previously[6] were used to correlate compression set to failure via a helium leak test, which is the only defined failure criterion for the O-ring in a SAVY-4000 container. In those experiments, the compression set had to be estimated from the nominal initial O-ring thickness (as given by the manufacturer) and the nominal gland depth (as given in the SAVY-4000 1-Qt engineering drawings). This estimate gave errors in compression set of ~20% for the container aged at 210°C (which was the only container that failed the leak test) and led us to define the compression set limit for failure as 65%. To improve this correlation between compression set and leak test failure, we repeated the whole container aging experiments with four containers at 210°C in FY17.

4.1.1 Experimental

O-rings were greased with Dow Corning High Vacuum Grease and installed in four 1-Qt SAVY containers, and each was placed in an aging oven at a temperature of 210°C. Periodically, over the course of nine months, the containers were withdrawn from the ovens and allowed to cool to room temperature for leak testing and compression set measurements. Leak testing was performed first, and then the O-rings were removed and cleaned for compression set measurements. Finally, the O-rings were re-greased and re-installed, and leak testing was performed again. After these measurements,the SAVY containers were placed back in the 210°C oven for further aging.

The leak rate of a SAVY-4000 container with the sample O-ring installed was measured using a LACO Flexstation™ bell-jar helium mass-spectroscopy leak tester. The leak tester detects the presence of a leak, defined as a rate higher than 1×10^{-5} atm cm^3 s^{-1}, by analyzing the atmosphere for helium in a bell jar held near vacuum, when the container in the bell jar is charged with 75 torr of helium.

Compression set measurements were conducted as per method B as described in the ASTM standard.[7] Each O-ring was cleaned to remove the grease and then measured for thickness using a laser micrometer, the optoCONTROL ODC2500-35. The compression thickness was taken as the gland depth calculated from CMM measurements taken during manufacturing. The thickness of each O-ring was measured with the LaserMike laser micrometer, as the average of eight measurements from around the O-ring. The amount of compression set was computed as

$$C_B = \frac{t_0 - t_i}{t_0 - t_n}$$

where C_B is the method-B compression set, t_0 is the original thickness, t_i is the final thickness, and t_n is the compression thickness.

4.1.2 Results

Figure 4.1a shows the average compression set and leak rate results as a function of aging time at 210°C, and Table 4.1 summarizes these data. At an aging time of 1300 hrs, the compression set approaches the failure criterion of 65%, but all cans pass the leak test, both before and after O-rings were removed and re-installed. At 4930 hrs, the average compression set (over all containers) is 84% ± 2%, and all four containers still pass the leak test. Finally, at 5100 hrs, the average compression set is 90% ± 2%, and we begin to see failures in the leak test: two containers failed before O-ring removal and re-installation, and one failed afterward. Thus, the removal and re-installation process improved the ability of the O-ring to maintain a proper seal in one of the failed containers, but not the other. Figure 4.1b plots the leak rate as a function of compression set: although no correlation can be observed, the three leak rate failures all had compression set values greater than the 65% failure criterion.

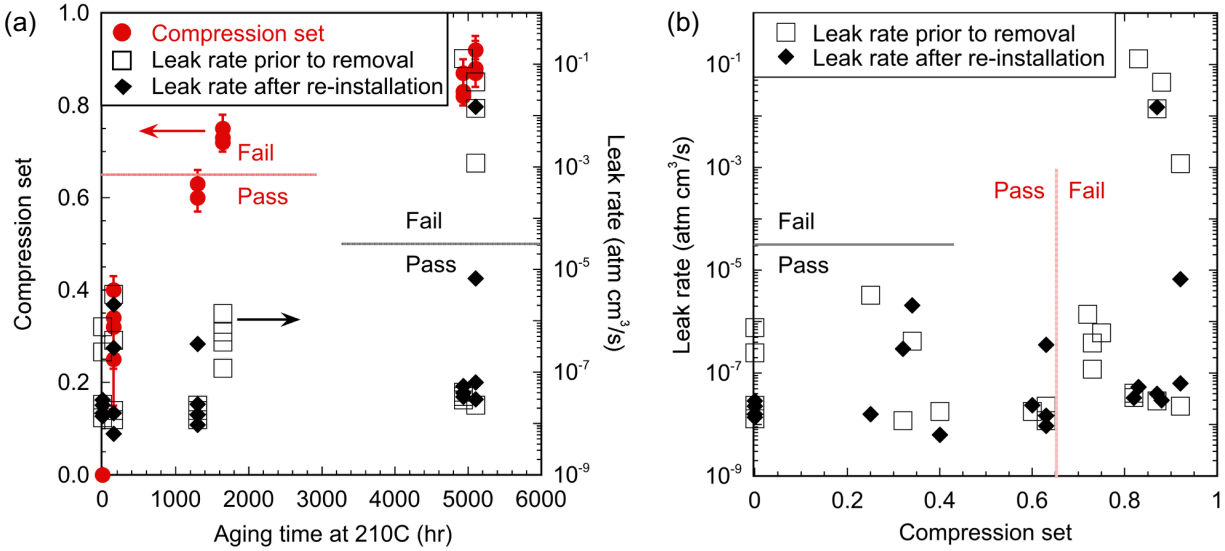

Figure 4.1. (a) Compression set (red circles) and leak rates (black diamonds and squares) for O-rings in whole containers aged at 210°C for 0 – 5100 hrs. (b) Data from (a) plotted as leak rate vs. compression set.

Table 4.1. Compression set (averaged over all four containers) and leak test results for the whole-container 210°C-aged O-rings.

Aging Time (hrs)	Compression Set	Leak Test Results Before O-ring Removal	Leak Test Results After O-ring Removal & Re-Installation
150	33% ± 7%	All Passed	All Passed
1300	63% ± 3%	All Passed	All Passed
1640	73% ± 2%	All Passed	All Passed
4930	84% ± 2%	All Passed	All Passed
5100	90% ± 2%	2 Passed; 2 Failed	3 Passed; 1 Failed

4.2 Solvent Swelling to Determine Degree of Crosslinking

4.2.1 Experimental

Crosslinked polymers are often evaluated via a solvent swelling technique in order to determine the molecular weight between crosslinks (M_c).[8]

M_c was determined by immersing the O-ring samples in a good solvent and then relating the equilibrium amount of solvent uptake to the relative amount of crosslinks. Approximately 1g of each O-ring sample was placed in a scintillation vial with tetrahydrofuran (THF). At various time points, the O-ring was removed and weighed. When its weight stopped changing (usually by 140 hrs of immersion), the sample was at equilibrium with the solvent. At this point, M_c was calculated as follows:

$$M_c = \frac{-\rho V_1 v_2^{1/3}}{K v_2^2/2 + \ln(1 - v_2) + v_2}$$

where ρ is the density of the O-ring polymer (1.86 g/mL), V_1 is the molality of the THF solvent (79.76 mL/mol), v_2 is the volume fraction of polymer in the swollen system, and K is the polymer-solvent interaction parameter. The polymer-solvent interaction parameter has not been measured for this system; thus, for the calculations herein, we used an estimated value of 0.5, based on literature results for a similar fluorocarbon copolymer.[9] While a different value for K would yield different absolute values of M_c, the trends reported below would not be altered. v_2 is calculated from the initial (m_i) and swollen (m_f) masses of the sample:

$$v_2 = \frac{m_i/\rho}{m_i/\rho + (m_f - m_i)/\rho_s}$$

where ρ_s is the density of the solvent (0.904 g/mL).

4.2.2 Results for Pristine O-ring Pieces

To obtain a baseline M_c value for unaged O-rings, samples were cut from pristine O-rings that represented four SAVY container sizes and three O-ring batch numbers / cure dates. Table 4.2 lists the sizes, batch numbers, and M_c results for these pristine samples. First, we note that the M_c values for the pristine 1-Qt O-ring are significantly lower than those found for 5-Qt, 8-Qt, and 10-gal O-rings. Interestingly, the batch number for the 1-Qt samples is the same as that for 8-Qt samples. This suggests that O-ring production processing conditions are different for the 1-Qt O-rings. A larger study would be needed to determine how widely M_c values differ for different batch numbers and sizes. For the current study, we assume that the M_c values listed in Table 4.2 for a given size are representative of all pristine O-rings of that same size.

Table 4.2. Sample information and M_c results for pristine O-ring pieces evaluated by solvent swelling.

Sample Name	Size	Batch Number	M_c (g/mol)
1-Qt A	1-Qt	81024905	35157
1-Qt B	1-Qt	81024905	34338
5-Qt A	5-Qt	81022913	46075
5-Qt B	5-Qt	81022913	45730
8-Qt A	8-Qt	81024905	48072
8-Qt B	8-Qt	81024905	49705
10-Gal A	10-Gal	81022755	45570
10-Gal B	10-Gal	81022755	45286

4.2.3 Results for Thermally Aged O-ring Pieces

Some of the O-ring pieces from the 3-year thermal accelerated aging study were evaluated via solvent swelling. During that accelerated aging study, each of these samples was held under compression for a given aging time at an elevated temperature between 70 and 210°C. The samples were stored at ambient conditions following their removal from the aging ovens and compression jigs. Table 4.3 give details regarding the samples used for the solvent-swelling experiments, along with the M_c values calculated from the results. The first entry in the table represents an average M_c for pristine O-rings; this value (47 ± 2 kg/mol) was calculated from the M_c values of the pristine O-ring pieces taken from 5-Qt, 8-Qt, and 10-Gal O-rings (as reported in Table 4.2). The aged O-ring pieces were originally taken from primarily from 5-Qt, 12-Qt, and 10-Gal O-rings, although this information was not recorded for some of the samples (see Table 4.3).

Figure 4.2a plots M_c vs. aging time. Generally, as aging time and temperature increase, M_c decreases, indicating that degradation of the O-ring is occurring through a crosslinking reaction. Interestingly, samples aged at 70 – 120°C appear to maintain a fairly constant M_c until dropping precipitously as aging time increases beyond 1000 hrs, while those aged at 160 – 210°C appear to decrease steadily until reaching a lower bound at $M_c \approx 28$ kg/mol. Beyond this lower bound, M_c begins increasing dramatically in samples aged at these high temperatures and longer aging times, suggesting that a chain scission mechanism begins to dominate. These samples did maintain their general shapes during the swelling experiments, indicating that the overall network structure was still intact. However, if chain scission continued further, the network structure would eventually be destroyed and the O-ring would be expected to crumble (though these samples did not).

For the samples that degrade through the crosslinking mechanism, the network becomes denser over time. Since the O-rings were aged under compression, these additional crosslinks also serve to lock in the compressed network structure, leading to increased compression set. This relationship can be seen in Figure 4.2b: as M_c decreases from ~47 kg/mol (for the pristine sample) to ~28 kg/mol, compression set increases in a dramatic, nonlinear fashion. However, compression set also increases dramatically for the samples dominated by chain scission. Here, the elastic restoring force due to the network structure has been degraded by the chain scission process, resulting in a large compression set.

Table 4.3. Accelerated aging conditions and M_c results for the 3-year accelerated aging study samples that were subsequently evaluated by solvent swelling.

Aging Temperature (°C)	Aging Time (hrs)	O-ring Size	Batch Number	"Relaxed" Compression Set	M_c (g/mol)
Ambient	0				46,740 ± 1761
70	0.5	5-Qt	80147869	0.01	42,861
	20	5-Qt	80147869	0.01	43,685
	50	5-Qt	80147869	0.01	43,935
	100	5-Qt	80147869	0.03	45,015
	4914	12-Qt	80152764	0.08	36,571
	5800	Not recorded	Not recorded	Not recorded	34,986
90	0.5	5-Qt	80147869	0.05	44,342
	5	5-Qt	80147869	0.01	44,877
	9	5-Qt	80147869	0.01	44,627
	50	5-Qt	80147869	0.04	45,501
	4878	12-Qt	80152764	0.09	34,674
120	2466	5-Qt	81022913	0.07	44,549
	4887	10-Gal	80152764	0.17	41,657
160	50	12-Qt	80152764	0.04	36,324
	3740	5-Qt	81022913	0.42	28,317
	13656	12-Qt	80152764	0.41	29,450
	22909	12-Qt	80152764	0.60	28,444
175	66	Not recorded	81022913	0.10	32,937
	144	5-Qt	81022913	0.16	35,909
	445	5-Qt	81022913	0.22	32,937
	1012	5-Qt	81022913	0.35	31,212
	3740	5-Qt	81022913	0.53	27,521
	4795	12-Qt	80152764	0.41	30,988
190	1	5-Qt	81022913	0.06	43,430
	11	Not recorded	Not recorded	0.04	37,427
	46	Not recorded	Not recorded	0.05	37,995
	988	Not recorded	Not recorded	0.35	30,501
	2320	5-Qt	81022913	0.22	28,579
	4794	12-Qt	80152764	0.68	34,819
210	0.6	5-Qt	81022913	-0.01	49,216
	24	10-Gal	80152764	0.12	44,978
	48	10-Gal	80152764	0.09	43,470
	98	5-Qt	81022913	0.32	34,568
	1414	5-Qt	81022913	Not recorded	62,904
	2867	5-Qt	81022913	0.95	61,507

In summary, these solvent-swelling experiments confirm that at least two chemical degradation mechanisms occurred in the accelerated aging study. One mechanism leads to crosslinking, and the other results in chain scission. Both contribute to compression set. However, chain scission is probably more detrimental to the lifetime of the O-ring because it destroys the elastic restoring force needed for the O-ring to form a seal.

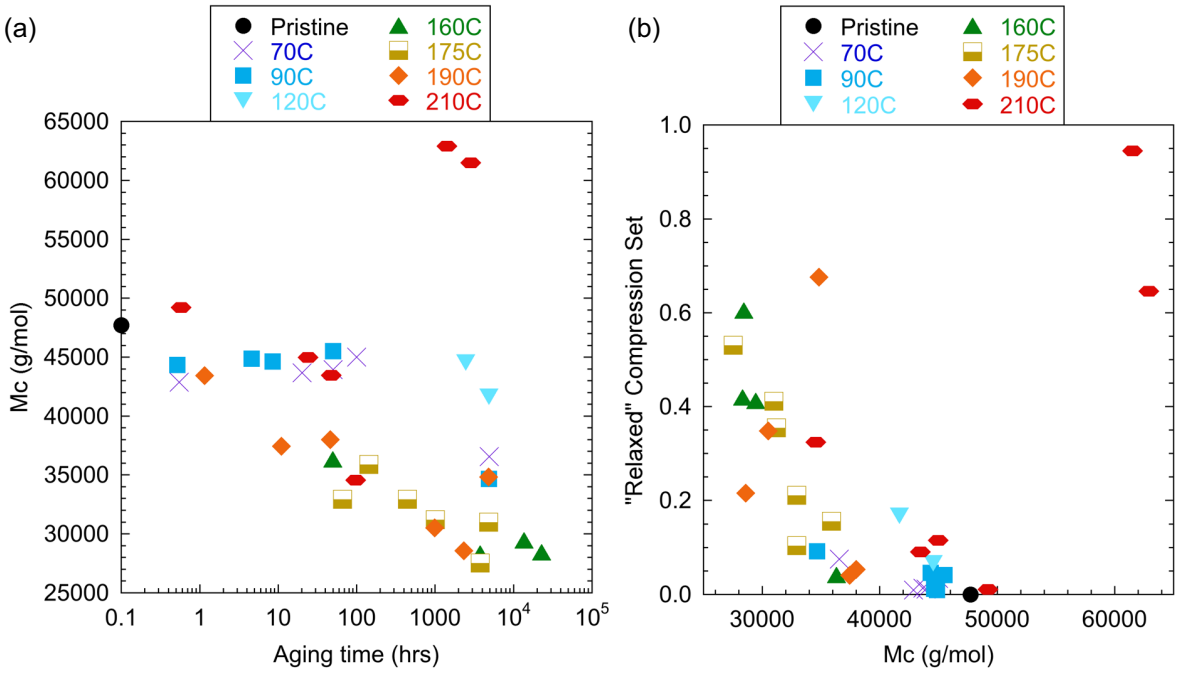

Figure 4.2. (a) Dependence of M_c on aging time and temperature; (b) Dependence of compression set on M_c.

4.2.4 Results for O-rings from Thermally Aged Whole Containers

At the conclusion of the whole-container thermal aging study described in Section 4.1, the O-rings were removed from the containers and cleaned. Then pieces were cut from these 1-Qt O-rings for solvent-swelling experiments. Table 4.4 lists the M_c results for these samples, along with the average value for a pristine 1-Qt O-ring (taken from Table 4.2). Each of the O-rings taken from the thermally aged whole containers have a significantly larger M_c value than the pristine sample, suggesting a chain scission degradation mechanism. In addition, compression set values were quite high, and some of these containers failed the leak tests reported in Section 4.1.

Table 4.4. Accelerated aging conditions and M_c results for the samples taken from O-rings in the whole-container thermal aging study.

Aging Temperature (°C)	Sample Name	Aging Time (hrs)	Compression Set	M_c (g/mol)
Ambient	Pristine	0		34,747 ± 579
210	WA	5100	0.92	60,850
	WB	5100	0.92	47,481
	WC	5100	0.88	44,829
	WD	5100	0.87	47,659

4.3 Oxygen Consumption

The data from the 3-yr accelerated aging study[6] suggested that at least two irreversible aging mechanisms occur in the SAVY O-rings. The solvent-swelling results above further demonstrate that one of these mechanisms results in further crosslinking of the network, while the other causes chain scission or destruction of the network. Possible chemical mechanisms include reaction of the polymer with the catalyst and / or other additives in the O-ring. Oxidation of the

polymer may also be occurring, and this process may be affected by the diffusion rate of oxygen into the O-ring. In FY17, we used a set of ultrasensitive oxygen consumption measurements under accelerated aging conditions[10,11,12] to investigate these possibilities. Since a report[13] was issued earlier in 2017 with all of the details of those experiments, we only give a brief summary here.

For this study, cross-sections of an O-ring for a 5-Qt SAVY container (batch number 0081022913) were cut to give cylindrical pieces with a thickness of 2 mm and diameter of 5.2 mm. To minimize the effects of diffusion-limited oxidation, these cross-sections were further cut into fourths. These O-ring sample pieces were placed in baked-out Swagelok sample chambers and then vacuumed and backfilled with compressed analyzed air (21.29% v/v oxygen). Next, the chambers were subjected to accelerated aging at seven temperatures (38°C, 50°C, 70°C, 90°C, 120°C, 160°C, and 210°C) for times ranging from 1 – 150 days. After aging, each sample chamber was connected to an Oxzilla dual-channel differential oxygen analyzer to measure any changes in oxygen concentration that occurred during the aging process. During this measurement, oxygen concentration is recorded as a function of time as air with a known oxygen content is flowed through the sample chamber. From this data, oxygen consumption was calculated as the integral under the peak of the oxygen concentration vs. time curve ($\int [O_2] dt$).[14] An oxygen consumption rate was then calculated to provide a quantity normalized against sample mass ($m \sim 2.5$ g), aging time (t_a), and volumetric gas flow rate ($\dot{V} = 0.5$ L/min):

$$\text{Oxygen consumption rate} = \frac{\dot{V} \int [O_2] dt}{m t_a} \ .$$

The results are plotted in Figure 4.3. At all aging temperatures, we see a high initial oxygen consumption rate that drops rapidly as aging time increases, and there is no apparent effect of aging temperature. Both of these trends are unusual. Oxygen consumption rate is normalized against time and, therefore, should be constant as aging time increases. Also, oxidation reactions usually require an activation energy; thus, higher temperatures usually enable faster oxygen consumption. The range of values observed for oxygen consumption rate is also somewhat unusual. Though literature results are limited, oxygen consumption rates for polymeric elastomers generally range from 10^{-14} to 10^{-9} mol/g-s.[10,11,15,16] The oxygen consumption rates observed at early aging times in Figure 4.3 are above this range, spanning from 10^{-7} to 10^{-9} mol/g-s for aging times of 1 – 10 days. The rates at the longest aging times (100 – 150 days) are in line with those observed for a similar Viton-like elastomer, although that study used a combination of radiation and elevated temperature to age the material.[15]

There may be multiple processes that contribute to produce these unexpected results. First, in spite of our efforts to eliminate diffusion-limited oxidation, the high initial rate of consumption could be due to diffusion processes. Second, two processes could be occurring: an oxygen-consumption process followed by an oxygen-generation (or other gas-generation) process. Third, a minor component in the O-ring (catalyst, filler, etc) could be undergoing oxidation to give the high consumption rates at early times; after this minor component fully oxidizes, the remaining oxygen consumption that we measure is due to the polymer. Fourth, there could be an induction period associated with the oxidation reaction.[10] Additional experiments would be necessary to positively identify or eliminate each of these possibilities.

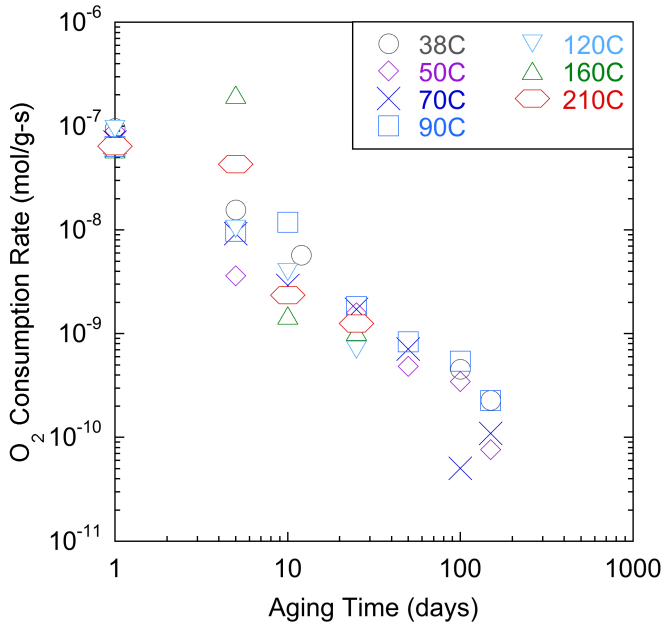

Figure 4.3 Oxygen consumption rate for O-ring pieces aged from 38 – 210°C and 1 – 150 days.

4.4 Synergistic Effects: Accelerated Aging with Radiation and Temperature

All results described above pertain to thermal aging alone, but we also need to understand how the O-ring behaves when subjected to radiation and elevated temperature simultaneously. As a continuation of synergistic effects experiments conducted in FY15,[17] we conducted additional experiments in June 2017 at the Gamma Irradiation Facility (GIF) at Sandia National Laboratory in Albuquerque.

4.4.1 Experimental

Four ovens were placed at four different locations within the GIF cell to obtain four dose rates from the cobalt 60 source: 4.32, 4.76, 6.00, and 9.94 rad/s. Samples were exposed to the source for 72 hours at a given temperature to give total doses of 1.12, 1.23, 1.56, and 2.58 Mrad, repsectively. For each 72-hour period, all ovens were set to the same temperature (20, 70, 160, or 210°C). At the end of the 72-hour period, samples were removed and evaluated as described below. Then all four ovens were set to the next test temperature and allowed to equilibrate before the next sets of samples were placed inside. Unfortunately, at some point during the 70°C experiment the ovens tripped the breaker; thus, this "temperature" is actually a gradient from 70°C to room temperature (20°C) over a 72-hour period.

Samples included as-received and annealed O-ring pieces (cut from 5-Qt O-rings, batch # 81004720) in compression jigs and 1-Qt SAVY containers with installed O-ring and filter. As-received O-ring pieces were 1-in long, and annealed pieces were 1.5-in long. Annealing was done at LANL prior to traveling to the GIF and was accomplished by placing uncompressed O-ring pieces in a 210°C oven for 72 hrs. Measurements taken before and after annealing revealed no significant changes in sample thickness or hardness: the average change in thickness was 0.009 mm (maximum 0.088 mm), and the average change in hardness was 0.15 (maximum 4.00).

Both annealed and unannealed O-ring pieces were greased before placing in the compression set jigs at the GIF. Whole O-rings used in the 1-qt SAVY containers were not annealed but were greased prior to installation in the container.

Compression set jigs used at the GIF were designed so that multiple jigs could be set in an aging oven during the experiment. The jigs were each 3 inches in diameter, and machined from 316 stainless steel. The chromium plate was omitted. The jig plates were held together with three nuts and bolts, and separated with the same 4-mm spacers used in the thermal aging compression set experiments. The jigs were heated to the oven temperature and then the samples were added. For each temperature / dose rate combination, three as-received and three annealed O-ring pieces were placed in a single compression jig. Each jig was compressed, and reintroduced to the oven. The source was then raised to begin the 72-hr exposure at that temperature.

After irradiation, the O-ring pieces were removed from the compression jigs and the whole O-rings were removed from the 1-qt SAVY containers. Whole O-rings and O-ring pieces were cleaned to remove the sealing grease. Each sample was then measured for compression set (in the same manner as described in Section 4.1.1 above) and hardness. The hardness of each sample was measured as described in the ASTM standard for durometry.[18] Our durometer is a Shore-M model 100 durometer, with a digital readout and hydraulic descent control. A stage extender was utilized with whole O-rings to make sure they could lie flat during measurement.

The filter from the SAVY container was also tested for water penetration, using a sealed system that allows air pressure to be applied to a column of water so that the desired water pressure can be reached. A mechanical fixture with an O-ring seal attached to the four threaded holes in the filter portion of the SAVY-4000 lid was used in conjunction with a measurable water column to test the water resistance function. The failure criteria for the water penetration test is the visual appearance of water at the lower surface of the filter when exposed to a 12-inch water column for a dwell time of one minute.

After these measurements, the 1-Qt SAVY containers were reassembled with the same O-ring (after applying new grease) and filter and then placed back in the ovens at the next temperature, along with fresh O-ring pieces within the compression jigs. In this way, the whole O-rings and filter received total doses of 4.48, 4.94, 6.22, and 10.3 Mrad, depending on the oven location. Each whole O-ring and filter experienced a temperature profile of 72 hrs at 20°C, 72 hrs at 70°C, 72 hrs at 160°C, and 72 hrs at 210°C.

When all of the GIF exposures were completed, all samples were brought back to LANL for additional measurements. The whole cans were leak-tested (in the same manner as described in Secion 4.1.1), compression set was measured for the O-rings, and leak testing was performed again after the O-ring was re-inserted. For the O-ring pieces aged in compression jigs, one unannealed sample piece for each aging condition (temperature, dose) was used for solvent swelling experiments (as described in Section 4.2.1).

4.4.2 Results: Compression Set of O-ring Pieces

Figures 4.4a and 4.4b show the compression set measured as a function of aging temperature and dose, respectively, with open markers for annealed samples and filled markers for unannealed samples. Both factors cause an increase in compression set, but no difference can be observed between annealed and unannealed samples.

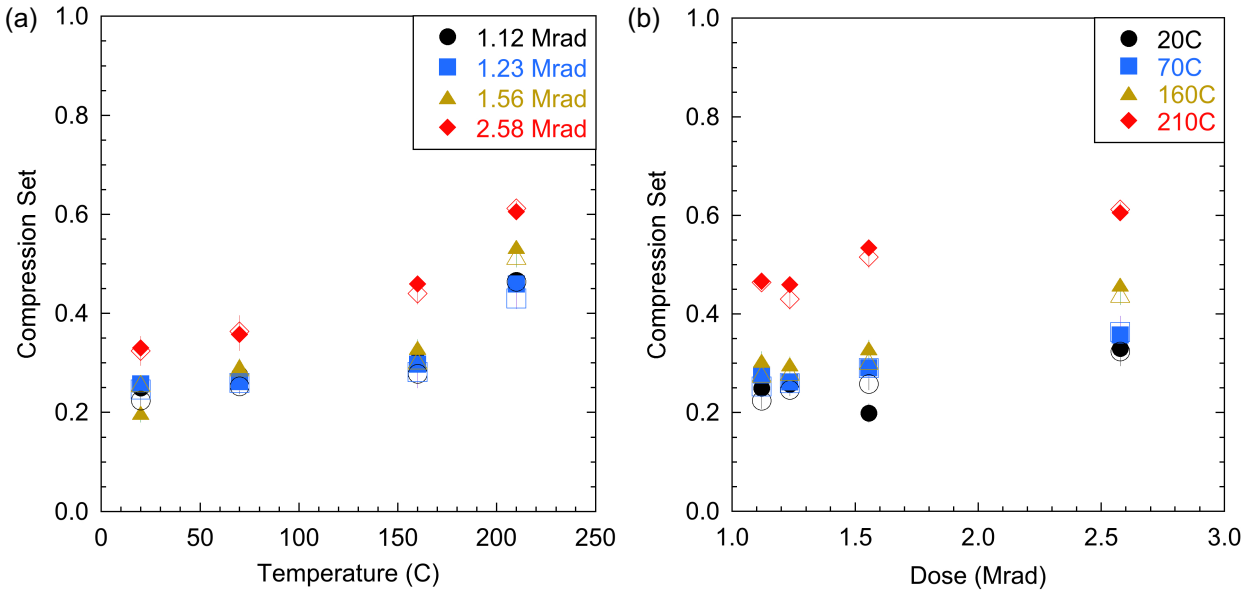

Figure 4.4. Compression set for O-ring pieces as a function of (a) temperature and (b) total dose for samples exposed to both elevated temperature and radiation at the GIF. Filled markers correspond to unannealed samples, while open markers are for annealed samples.

To determine if there is a synergistic effect between temperature and radiation with respect to compression set, a two-way analysis of variance (ANOVA) was performed on the data from the unannealed experiments and from the annealed experiments separately. For these analyses, temperature and dose are the factors and compression set is the response; the results are reproduced in Tables 4.5 and 4.6. In these tables, the values for "Sum_sq," "F," and "ω^2" can be used to determine if a factor (temperature or dose) has an effect on the response (compression set); for each of these, higher values indicate greater effects. "Sum_sq" is the sum, over all observations, of the squared difference of each observation from the overall mean. "F" compares the sum of squared values to the "Residual," which represents the error (or noise) in the model. "ω^2" estimates the effect size by calculating the variance in the response; a value of zero indicates that the factor does not affect the response. "Df" represents the degree of freedom (or the number of values that are independent from each other), while "p" compares the data for a given factor to the "Residual." A p-value of 0.01 corresponds to a 99% confidence range.

Table 4.5. ANOVA for compression set on unannealed O-ring pieces.

	Sum_sq	Df	F	p	ω^2
Temperature	1.4013	3.0	414.7551	1.0×10^{-65}	0.7059
Dose	0.3666	3.0	108.5173	5.3×10^{-35}	0.1834
Temp:Dose	0.0670	9.0	6.6106	1.0×10^{-7}	0.0287
Residual	0.1442	128.0			

For the unannealed samples, the ANOVA shows a significant effect for temperature, dose and the combined effects of temperature and dose on the compression set attained during each experiment, because the p-value for each is much smaller than the typical 0.05 value. The effect size, conservatively estimated as ω^2, however, shows that the temperature has a greater effect on

the compression set than the dose. Moreover, the independent effects of temperature and dose are greater than the synergistic effect of both.

Table 4.6. ANOVA for compression set on annealed O-ring pieces.

	Sum_sq	Df	F	p	ω^2
Temperature	1.3508	3.0	348.4520	2.3×10^{-61}	0.6811
Dose	0.4263	3.0	109.9740	2.9×10^{-35}	0.2136
Temp:Dose	0.0337	9.0	2.9004	3.7×10^{-3}	0.0112
Residual	0.1654	128.0			

For the annealed samples, the significance of the effect is about the same as for the unannealed samples, as is the effect size. The p-value for the synergistic effect is much larger than the rest, though it is still below the typical 0.05 cutoff.

Given that there is a weak synergistic effect, we can find an equation describing the relationship between compression set C_B (as a fraction), temperature (T in °C) and dose (D in Mrad) by performing a non-linear least-squares fit of the function below to the experimental data:

$$C_B = F(T, D) = a + b(T) + c(D) + d(T * D)$$

For unannealed samples, the coefficients are $a = 0.12 \pm 0.03$, $b = 0.0008 \pm 0.0002$, $c = 0.06 \pm 0.02$, and $d = 0.0003 \pm 0.0001$. For the annealed samples, the coefficients are $a = 0.11 \pm 0.03$, $b = 0.0007 \pm 0.0002$, $c = 0.06 \pm 0.02$, and $d = 0.0003 \pm 0.0001$. There are no substantial differences between the annealed and unannealed results.

4.4.3 Results: Hardness of O-ring Pieces

Figures 4.5a and 4.5b show the change in hardness measured as a function of aging temperature and dose, respectively, with open markers for annealed samples and filled markers for unannealed samples. The values shown are averages taken over 9 measurements (3 readings for each of the 3 replicates), and error bars reflect the standard deviation. As temperature increases (Figure 4.5a), the change in hardness appears to slightly decrease at all doses; a negative change in hardness means that the samples became softer. In Figure 4.5b, no clear trends are discerned; change in hardness appears to be independent of dose, at least within the error of the measurement. In both figures, no difference can be observed between annealed and unannealed samples.

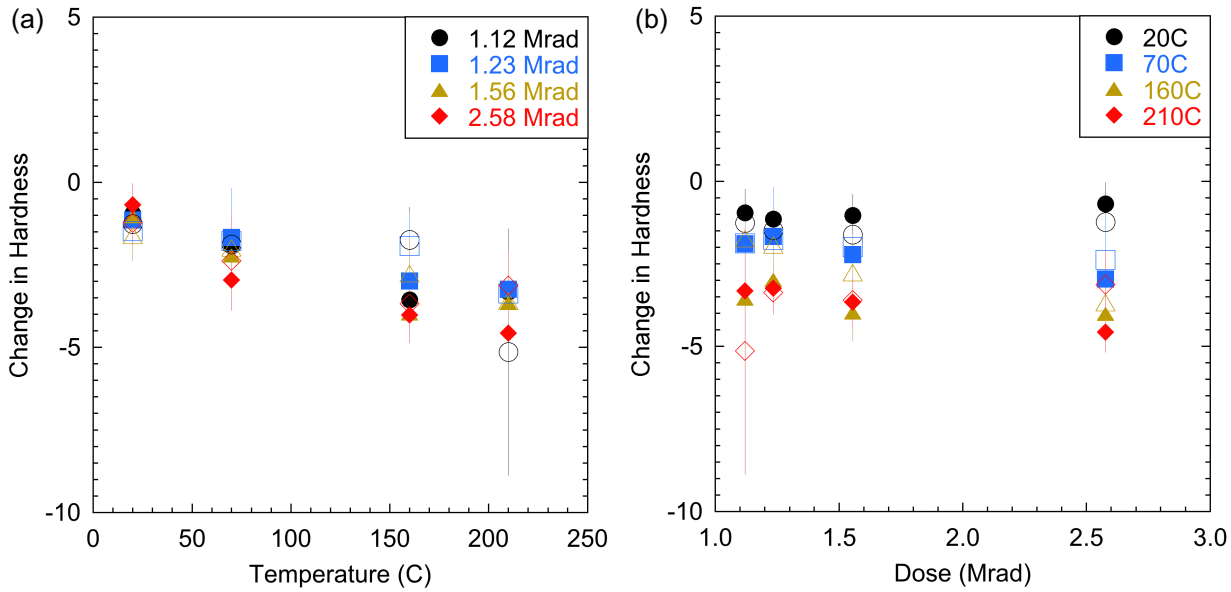

Figure 4.5. Change in hardness for O-ring pieces as a function of (a) temperature and (b) total dose for samples exposed to both elevated temperature and radiation at the GIF. Filled markers correspond to unannealed samples, while open markers are for annealed samples.

4.4.4 Results: Solvent Swelling of O-ring Pieces

Figures 4.6a and 4.6b show the molecular weight between crosslinks measured as a function of aging temperature and dose, respectively. Recall that M_c for an unaged sample is ~47 kg/mol; therefore, exposure to the combination of elevated temperature and radiation results in lower M_c values (and a higher degree of crosslinking) for all samples shown in Figure 4.6. Somewhat counterintuitively, Figure 4.6a shows that higher temperatures yield higher M_c values, or a smaller difference in M_c compared to the pristine sample. We see the opposite trend with dose: M_c generally decreases as dose increases, though the effect of dose on M_c becomes smaller as temperature increases.

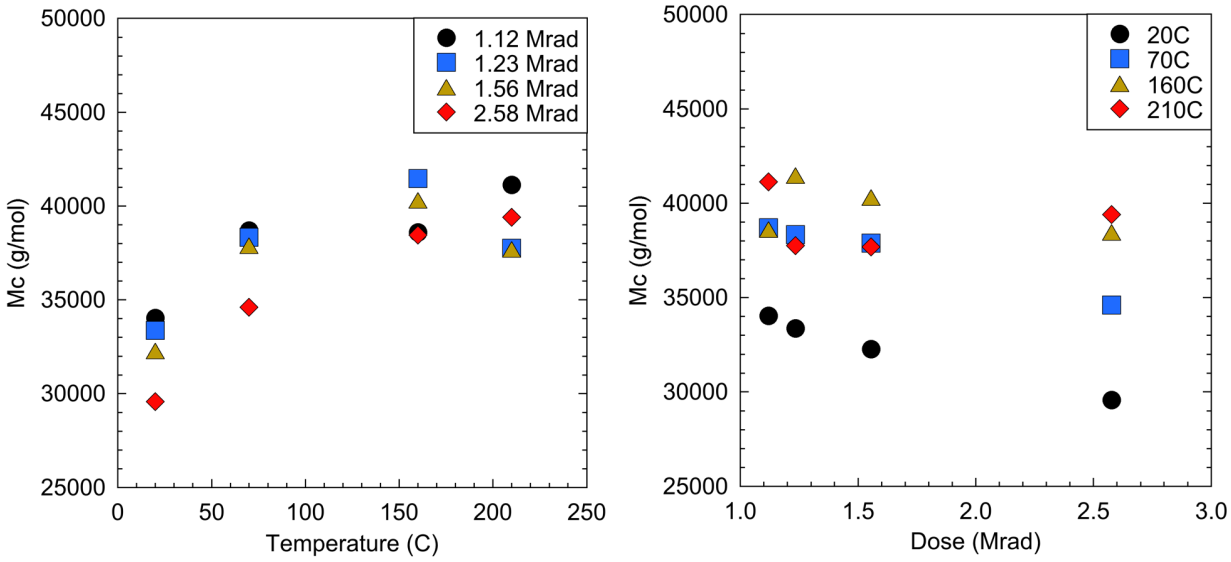

Figure 4.6. Molecular weight between crosslinks as a function of (a) temperature and (b) total dose for unannealed samples exposed to both elevated temperature and radiation at the GIF.

In Figure 4.7, we attempt to understand the effect of changes in M_c on compression set. At a given total dose (Figure 4.7a), compression set generally increases with M_c, but the changes in compression set are fairly minimal except for samples exposed to the highest dose (2.58 Mrad). In Figure 4.7b, the data points are generally clustered for a given temperature, which suggests that temperature has a larger effect on the relationship between compression set and M_c, compared to the effect that total dose has.

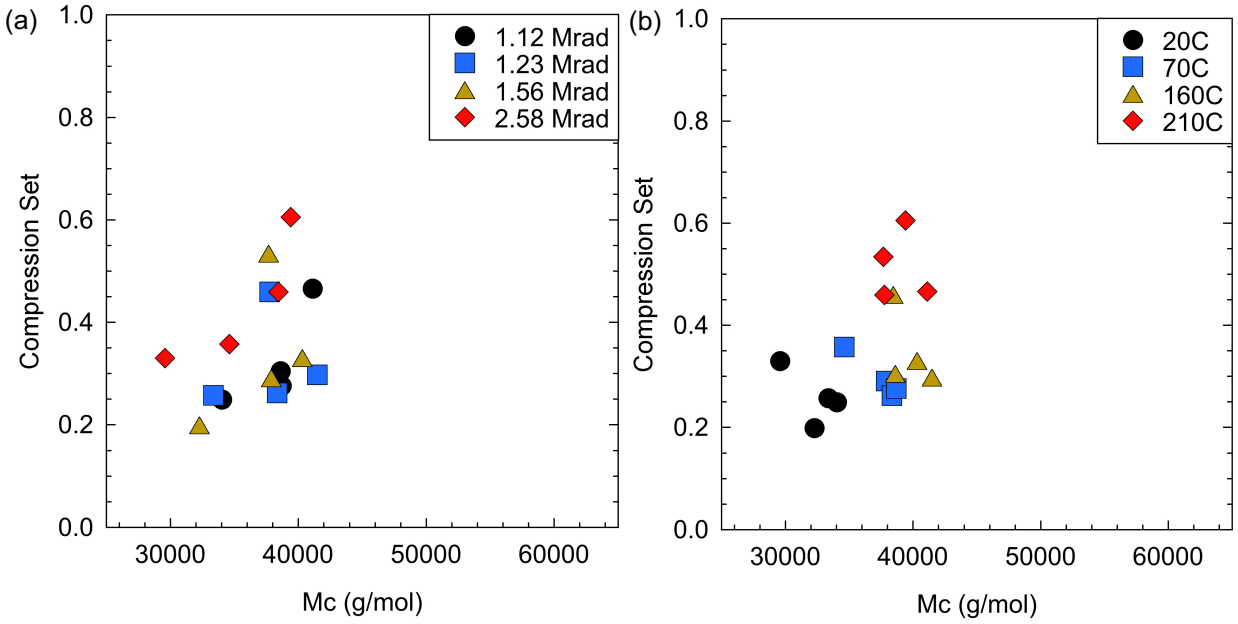

Figure 4.7. The effect of M_c on compression set for unannealed samples exposed to both elevated temperature and radiation at the GIF. In (a) data points are grouped according to total dose, while (b) groups them according to temperature.

4.4.5 Results: Whole Container O-rings

Each of the four whole 1-Qt containers were exposed to a temperature profile of 72 hrs at 20°C, 72 hrs at 70°C, 72 hrs at 160°C, and 72 hrs at 210°C. The four containers experienced different dose rates, depending on oven location. After each 72-hr period at a given temperature, the O-rings were removed from the whole containers, tested for compression set and hardness, and then returned to the same whole container and oven/dose rate location. Table 4.7 shows the progression of temperature and total dose for each container, along with measurement results obtained after each 72-hr period.

Figure 4.8a shows that compression set increases with total dose in a fairly steady fashion for the whole O-rings. The 20°C data can also be compared to that of the O-ring pieces (from Figure 4.4b), and this is shown in Figure 4.8b. No significant differences can be observed between the whole O-rings and the O-ring pieces.

Table 4.7. Sample details and measurement results for O-rings aged in 1-Qt SAVY containers at the GIF.

Sample	Total Dose (Mrad)	Total Aging Time (hrs)	Compression Set
A, after 20°C irradiation	2.58	72	0.37 ± 0.04
B, after 20°C irradiation	1.56	72	0.30 ± 0.04
C, after 20°C irradiation	1.23	72	0.26 ± 0.05
D, after 20°C irradiation	1.12	72	0.25 ± 0.04
A, after 70°C irradiation	5.15	144	0.38 ± 0.06
B, after 70°C irradiation	3.11	144	0.43 ± 0.05
C, after 70°C irradiation	2.47	144	0.27 ± 0.09
D, after 70°C irradiation	2.24	144	0.26 ± 0.10
A, after 160°C irradiation	7.73	216	0.66 ± 0.04
B, after 160°C irradiation	4.67	216	0.60 ± 0.04
C, after 160°C irradiation	3.70	216	0.48 ± 0.06
D, after 160°C irradiation	3.36	216	0.50 ± 0.04
A, after 210°C irradiation	10.31	288	0.89 ± 0.04
B, after 210°C irradiation	6.22	288	0.83 ± 0.04
C, after 210°C irradiation	4.94	288	0.72 ± 0.05
D, after 210°C irradiation	4.48	288	0.75 ± 0.03

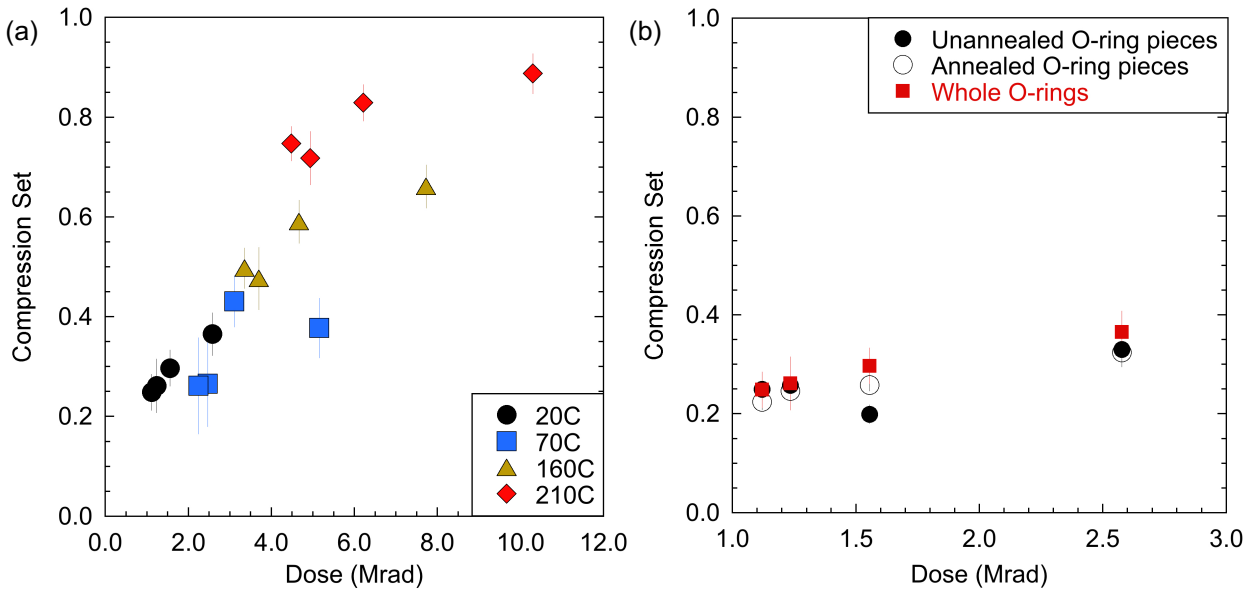

Figure 4.8. Compression set as a function of total dose for (a) whole O-rings aged in 1-Qt containers with a temperature profile of 72 hrs at 20°C, 72 hrs at 70°C, 72 hrs at 160°C, and 72 hrs at 210°C; and (b) whole O-rings compared to O-ring pieces, all aged at 20°C.

Table 4.8 shows the final compression set and leak test results for the O-rings aged in the whole containers, both immediately after the entire set of GIF experiments (A, B, C, and D) and several months later (A post, B post, C post, and D post). Immediately after the GIF experiments, the containers with the two highest total doses (and highest compression set values) failed the leak

test, while the two containers with lower doses passed. Several months later (and after the O-rings had been removed, cleaned, re-greased and replaced in the containers), only the container with the highest total dose (container A) still failed the leak test. Within error, the compression set values did not change during this time period. Thus, the removal and replacement procedure enabled the O-ring in container B to maintain a proper seal, in spite of its large compression set. On the other hand, this procedure was not effective in producing a proper seal for container A, perhaps because of its slightly larger compression set. Interestingly, and perhaps coincidentally, the compression set for this failed O-ring (~90%) is the same as the average recorded for 1-Qt whole-container O-rings that were thermally aged at 210°C for 5100 hrs, the time at which leak test failures began to occur (see Section 4.1).

Table 4.8. Compression set and leak test results for O-rings aged in whole containers at the GIF.

Sample	Compression Set Result	Helium Leak Test	Helium Background (atmcc/sec)	Helium Leak Rate (atmcc/sec)	Total Dose (Mrad)
A	89% ± 4	FAIL	5.10E-07	8.30E-02	10.31
B	83% ± 4	FAIL	1.40E-07	4.50E-04	6.22
C	72% ± 5	PASS	7.80E-08	2.40E-08	4.94
D	75% ± 3	PASS	8.00E-08	2.70E-08	4.48
A post	90% ± 4	FAIL	1.00E-07	4.20E-03	10.31
B post	80% ± 4	PASS	8.70E-08	3.50E-08	6.22
C post	71% ± 6	PASS	9.80E-08	2.90E-08	4.94
D post	71% ± 4	PASS	9.70E-08	3.20E-08	4.48

4.4.6 Results: Whole Container Filters

The filters performed exceptionally well when exposed to the combined effects of temperature and radiation at the GIF. The whole container filter's water resistance did eventually fail at the extreme temperature of 210°C. This result was expected as the maximum operating temperature prescribed by the manufacturer is 130°C. The maximum gamma irradiation seen by the filters was 10.31 Mrad and the maximum exposure temperature where the membrane passed the water penetration test was 160°C. The filter particle penetration performance was also measured along with the pressure drop across the filter after the GIF tests. It should be noted that the manufacturer only tests the particle penetration to the passing criteria and terminates the test. The filters continued to perform to the design criteria after the GIF tests were complete. The 40 year dose is expected to not exceed 5 Mrad.[19] Therefore, a lifetime of 40 years based on radiation damage and heat are well within the limits of the membrane material to prevent water ingress.

Table 4.9. Production and Post-GIF experiments filter performance data of whole containers.

SAVY-4000 Serial Number	Production Filter Percent Particle Penetration	Post-GIF Experiment Filter Percent Particle Penetration	Production Filter Pressure Drop	Post-GIF Experiment Filter Pressure Drop
011701137 A	0.0190%	0.0007%	0.80 in. WC	0.338 in. WC
011701128 B	0.0090%	0.0008%	0.75 in. WC	0.350 in. WC
011701129 C	0.0010%	0.0004%	0.74 in. WC	0.353 in. WC
011701144 D	0.0190%	0.0000%	0.69 in. WC	0.338 in. WC

5 Discussion and Conclusions

The statistical model for the 3-yr accelerated thermal aging data in Section 3 and the new experiments in Section 4 all confirm the conclusions of the FY16 SAVY-4000 Lifetime Extension Report. Multiple aging mechanisms are operative, with some type of crosslinking reaction being the dominant mechanism over most aging conditions tested. At the highest aging temperature / time combinations, chain scission dominates and begins to destroy the network structure. Both the crosslinking mechanism and the chain scission reaction cause increased compression set, with chain scission leading to the most extreme values of compression set. O-ring samples exposed to both thermal and radiative aging conditions show a weak synergistic effect, but aging temperature is the dominant cause of compression set. Solvent-swelling experiments with thes samples showed that further crosslinking occurred, though aging time for the O-ring pieces in this synergistic study was limited to 72 hrs at a given dose and temperature. Whole cans aged either thermally or synergistically (thermal + irradiation) do not fail the leak test until a very high compression set is reached, in the vicinity of 80 – 90%. As shown in our previous report and as verified by the statistical modeling in Section 3, using 65% compression set as a failure criterion supports a lifetime of the O-ring of at least 40 years. As surveillance results are collected over the years to come, that lifetime could be extended further.

6 References

1) DOE, "Nuclear Material Packaging Manual." **DOE M 441.1-1,** https://www.directives.doe.gov/directives/current-directives/441.1-DManual-1/view
2) Smith, P.H.; Stone, T.A.; Veirs, D.K.; Anderson, L.L.; Blair, M.W.; Hamilton, J.; Kelly, E.; Moore, M.E.; Teague, J.G.; Weis, E.; Yarbro, T.F., DOE/NNSA review, "Safety analysis report for the SAVY 4000 container series" (2012).
3) Gladson, J.; Hagan, R., "Nuclear Material Container Testing," Los Alamos National Laboratory (1999).
4) Weis, E.M., Blair, M.W., Hill, B.D., Stone, T.A., Smith, P.H., Winter, J.C., Reeves, K.P., and Veirs, D.K., "Durability and field condition study of seal of SAVY-4000 storage container." (2014), Packaging, Transport, Storage & Security of Radioactive Material **25(1):** 24-9. 10.1179/1746510914y.0000000059
5) Blair, M.W., Weis, E., Veirs, D.K., Smith, P.H., Stone, T.A., and Ball, J.M., Service Life Prediction of Polymeric Materials: Vision for the Future ; 2013-03-03 - 2013-03-08 ; Monterrey, California, United States, "Accelerated Aging Studies for the Lifetime Extension of O-rings Used in the SAVY-4000 Unit," (2013).
6) Weis, E.M., Welch, C.F., Smith, P.H., Blair, M.W.; Stone, T.A.; Veirs, D.K.; Reeves, K.P.; Karns, T.; Oka, J.M.; Keller, J.; Meincke, L.; Torres, J.A.; Herman, M.J.; Weaver, B.; Adams, J.C.; Trautschold, O.C., "Lifetime Extension Report: Progress on the SAVY-4000 Lifetime Extension Program," Los Alamos National Laboratory report, LA-UR-16-27168 (2016).
7) ASTM International. *Standard Test Methods for Rubber Property — Compression Set*; ASTM D 395 – 03; 2008; Vol. 9.
8) Flory, P.J.; Rehner, J. *J. Chem. Phys.* **1943**, *11*, 521.
9) Okabe, M.; Wada, R.; Tazaki, M.; Homma, T., *Polymer Journal* **2003**, *35*, 798.
10) Wise, J.; Gillen, K.T.; Clough, R.L. *Polym. Degrad. Stab.* **1995**, 49, 403.
11) Assink, R.A.; Celina, M.; Skutnik, J.M.; Harris, D.J. *Polymer* **2005**, *46*, 11648.
12) Herzig, A.; Johlitz, M.; Lion, A. *Continuum Mech. Thermodyn.* **2015**, *27*, 1009.
13) Welch, C.F.; Keller, J.; Weis, E.; Adams, J.C.; Trautschold, O.C.; Stone, T.A.; Smith, P.H., "Oxygen Consumption Analysis of O-rings used in the SAVY-4000 Container under Accelerated Aging Conditions," Los Alamos National Laboratory report, LA-UR-17-26863 (2017).
14) To automate this process, a script in the R statistical programming language was written by Paul Welch (T-4) to determine the baseline signal in the data and integrate the peak due to oxygen consumption using the trapezoid rule.
15) Wise, J.; Gillen, K.T.; Clough, R.L., *Radiat. Phys. Chem.* **1997**, *49*, 565.
16) Gillen, K.T.; Bernstein, R.; Celina, M., *Rubber Chem. Tech.* **2015**, *88*, 1.
17) Weis, E.M.; Blair, M.W.; Herman, M.J.; Keller, J.; Torres, J.A.; Edwards, S.L.; Cordes, N.L.; Oka, J.M.; Karns, T.; Brown, A.D.; Veirs, D.K.; Smith, P.H.; Stone, T.A., "FY 2015 Annual Report: Progress on the SAVY-4000 O-Ring Certification and Lifetime Extension Program," Los Alamos National Laboratory Report (2015).
18) ASTM International. Standard Test Method for Rubber Property — Durometer Hardness. *Annual Book of ASTM Standards*, 2010, *D2240 – 5*, 1–13.
19) Cardon, R. A., "Polymer Seals in Radiological Service," Los Alamos National Laboratory Criterion 428 R1 (2010).